PETROVIETNAM
SCIENCE, TECHNOLOGY & INNOVATION

CONVERSION OF SUSTAINABLE AGRICULTURAL RESIDUES INTO MCC FOR PLA-BASED BIODEGRADABLE PLASTIC APPLICATIONS

Vu Thi Thu Ha, Nguyen Thi Bay, Nguyen Thanh Trung , Pham Nam Phong, Pham Van Bac, Nguyen Thi Thu Trang
National Key Laboratory for Petrochemical and Refinery Technologies
Email: ptntd2004@yahoo.fr
https://doi.org/10.47800/PVSI.2025.06-07

Summary

Microcrystalline cellulose (MCC) was extracted from cassava stems, banana pseudostems, pineapple leaves, and spent coffee grounds through an optimized acid hydrolysis process. Comprehensive structural, morphological, and thermal characterization revealed distinct differences among sources, with cassava stem-derived MCC identified as the most feasible and sustainable option due to its high crystallinity, uniform particle size, processing stability, ready availability, and large-scale supplypotential. This MCC was incorporated into thermoplastic starch (TPS) and polylactic acid (PLA) matrices to fabricate fully biodegradable composites. X-ray diffraction (XRD) confirmed the preservation of MCC crystalline structure, scanning electron microscopy (SEM) revealed homogeneous dispersion within the TPS phase, and thermogravimetric/differential thermal analyses (TGA/DTA) demonstrated improved thermal stability. Mechanical testing showed that the optimized PLA:MCC:TPS ratio of 70:4.5:25.5 (with 15% MCC relative to (MCC/TPS)) provided the best balance between tensile strength, modulus, and biodegradability.These composites exhibited mechanical strength for sustainable packaging and food service applications while maintaining full compostability. Overall, the results highlight cassava stems as a sustainable, locally available MCC source and confirm that PLA/(MCC/TPS) composites can replace petrochemical-based plastics in targeted sectors, contributing to global energy transition strategies and CO_2 emission reduction targets.

Key words: Agricultural residues, biomass-derived chemicals, biodegradable composites, cassava stems, energy transition, microcrystalline cellulose, polylactic acid.

1. Introduction

Agricultural residues such as cassava stems, banana pseudostems, pineapple leaves, and spent coffee grounds are abundant biomass resources that remain largely underutilized. These lignocellulosic wastes are rich in cellulose, a renewable biopolymer that can be transformed into microcrystalline cellulose (MCC) through relatively simple extraction processes. MCC is widely recognized for its high crystallinity, excellent reinforcing potential, and biodegradability, making it suitable for integration into biobased polymer composites [1 - 5]. Experimental studies have shown that incorporating microcrystalline cellulose (MCC) into PLA can significantly improve mechanical properties and thermal stability of PLA/MCC composites [6, 7]. These improvements demonstrate the potential of MCC as a sustainable reinforcement in PLA matrices, supporting development of renewable and eco-friendly bioplastics. Such composites align with global goals toward low-carbon, circular economies and enhanced performance of biodegradable materials in packaging and other applications.

In this study, MCC was extracted from four agricultural residues: cassava stems, banana pseudostems, pineapple leaves, and spent coffee grounds. A systematic comparison of their structural, morphological, and thermal properties identified cassava stem-derived MCC as the most feasible source, considering its high crystallinity, uniform particle morphology, thermal stability, abundant availability, and large-scale supply potential. This MCC was then incorporated into PLA/TPS blends to produce fully biodegradable biocomposites.

Given the global imperative to transition toward renewable, biomass-derived materials for both energy transition and CO_2 emission reduction, developing high-

Date of receipt: 19/8/2025
Date of review and editing: 19/8 - 15/10/2025
Date of approval: 15/10/2025

performance PLA/(MCC/TPS) composites from agricultural residues offers significant environmental and industrial advantages. This work aims to (i) valorize agricultural waste into value-added MCC; (ii) enhance the mechanical and thermal performance of PLA/TPS composites; and (iii) propose a sustainable pathway to replace petrochemical plastics in packaging and food service applications.

2. Materials and methods

2.1. Raw materials

Cassava stems, banana pseudostems, pineapple leaves, and spent coffee grounds were used for the extraction of microcrystalline cellulose (Figure 1). Cassava stems, banana pseudostems, and pineapple leaves were collected from local sources in Phu Tho and Thanh Hoa provinces, whereas spent coffee grounds were provided by Trung Nguyen Instant Coffee Joint Stock Company (Vietnam). After washing, cassava stems, banana pseudostems, and pineapple leaves were cut into 1 - 2 cm pieces; spent coffee grounds were used directly without further pretreatment. Thermoplastic starch was prepared in-house from avocado seeds (an agricultural waste source) by plasticization with glycerol and water, and was used without additional purification. Commercial PLA, glycerol (≥ 99%), and maleic anhydride (MA, ≥ 98%) were used as received.

2.2. MCC preparation

The extraction and isolation of MCC from the raw materials were carried out using the method described in [8], with process conditions modified for this study. Washed biomass was dried at 70 - 80°C, for 24 hours, milled, and sequentially treated with 0.1 N acetic acid and 15% NaOH (solid-to-liquid ratio of 1:20 g/ml, 105°C, 2 hours each), with washing to neutral pH. Bleaching with 3% H_2O_2 (1:10, 70°C, 4 hours) was followed by hydrolysis with 1.5 M HNO_3 (1:25, 70°C, 3 hours). MCC was washed to pH = 7, dried at 50°C for 24 hours, then milled, and stored.

2.3. MCC/TPS blends

The experimental preparation of thermoplastic starch and the MCC/TPS compound was conducted following the procedure described in [9]. Based on the components and mixing ratios reported in [9], the formulation and processing conditions were modified and optimized to obtain MCC/TPS composites suitable for the materials investigated and to achieve optimal performance. TPS was obtained by heating starch, glycerol, and water (30:40:30 wt%) at 120 - 130°C for 15 minutes with stirring. MCC (5 - 20 wt%) was incorporated, mixed at 80°C for 10 minutes, dried at 60°C for 6 hours), and cut for PLA blending.

2.4. PLA/(MCC/TPS) composites

PLA-MA was prepared by reactive melt-grafting of maleic anhydride (MAH, 3 wt% relative to PLA) in the presence of dicumyl peroxide (DCP, 0.2 wt%) at 190°C for 3 minutes in an internal mixer, following the procedure reported for PLA/MCC composites [10]. PLA-MA and MCC/TPS were dried at 60°C for 6 hours, weighed to the desired compositions (20 - 40 wt% MCC/TPS), and dry-mixed. Blending was carried out at 160 - 180°C for 10 - 15 minutes under stirring. The molten mixture was cast into non-stick aluminum molds, lightly pressed, cooled, demolded, cut, and dried at 50°C to remove residual moisture.

2.5. Characterization

FTIR spectra were recorded on a Nicolet 6700 (Thermo Electron) using KBr pellets (4000 - 400 cm^{-1}). XRD was performed on a D8 Advance (Bruker AXS) with Cu Kα radiation (λ = 1.5406 Å, 40 kV, 30 mA), 2θ = 5 - 40°, step size 0.02°, and the crystallinity index (CrI) was calculated using the Segal method. TG-DTA was conducted on a Diamond TG-DTA (Perkin Elmer) under nitrogen (RT-600°C, 10°C/min). SEM images were obtained using a Hitachi S-4800 at 10 - 15 kV after sputter-coating with gold.

2.6. Evaluation of performance and material properties

The actual yield of MCC relative to the raw material was calculated according to Equation (1).

$$Actual\ yield\ (\%) = \frac{M_2}{M_1} \times 100 \quad (1)$$

Where:

M_1 is the initial dry mass of raw material (g),

M_2 is the mass of MCC obtained (g).

The collection efficiency of MCC relative to the theoretical yield was determined using Equation (2).

$$Collection\ efficiency\ (\%) = \frac{M_2}{M_o} \times 100 \quad (2)$$

Where:

M_o is the theoretical mass of MCC in the raw material (g),

M_2 is the obtained mass of MCC (g).

The crystallinity of MCC was determined using the crystallinity index (CrI), calculated according to Equation (3).

$$CrI\ (\%) = \frac{(I_{200} - I_{am})}{I_{200}} \times 100 \quad (3)$$

Where:

CrI is the relative degree of crystallinity (%),

I_{200} is the maximum intensity of the (200) crystalline plane,

I_{am} is the intensity of the amorphous region.

2.7. Mechanical properties

Tensile strength and elongation at break were determined following TCVN or ASTM D638. Elastic modulus was measured using a universal testing machine under tensile-compressive loading. Standard dog-bone specimens were used.

3. Results and discussion

3.1. Recovery yield and structural characterization of MCC

The analytical results evaluating the composition and properties of the four biomass sources - pineapple leaves, banana pseudostems, cassava stems, and spent coffee grounds - are summarized in Table 1. The MCC recovery efficiency obtained from these biomass sources is presented in Table 2.

The results showed that the actual MCC yields obtained from pineapple leaves, banana pseudostems, cassava stems, and spent coffee grounds were 22.7%, 18.5%, 22.2%, and 10.4%, respectively. Corresponding collection efficiencies relative to the theoretical values ranged from 95.5% to 98.3%. Among the studied biomass sources, pineapple leaves and cassava stems exhibited the highest MCC yields (over 22%), followed by banana pseudostems (18.5%), whereas spent coffee grounds produced the lowest yield (10.4%). These differences can be attributed to the variations in the initial cellulose content and the extent of lignin and hemicellulose removal achieved during the chemical treatment process.

SEM micrographs further support these findings (Figure 3). Raw biomass samples such as pineapple leaf fibers and banana pseudostems (Figures 3a and 3c) display

Figure 1. *Raw material sources for MCC production: cassava stem, banana pseudostems, pineapple leaf, spent coffee grounds.*

Table 1. *Composition and properties of raw biomass materials (dry weight basis)*

Raw material sample	Cellulose (%)	Hemicellulose (incl. extractives) (%)	Lignin (%)	Ash (%)	Moisture content (%)
Pineapple leaves	23.7	56.0	16.4	3.9	5.7
Banana pseudostems	20	67.4	10	2.6	8
Cassava stems	23	45.9	26		7
Spent coffee grounds	11	56.3	27	5.7	8

Table 2. *MCC recovery yield from different biomass sources*

Raw material	Dry mass of raw material (g)	Mass of MCC obtained (g)	Actual MCC yield (%)	MCC collection efficiency compared to theory (%)
Pineapple leaves	102	23.2	22.7	97.8
Banana pseudostems	104	19.2	18.5	96.1
Cassava stems	102	22.6	22.2	98.3
Spent coffee grounds	101	10.5	10.4	95.5

compact, heterogeneous surfaces with visible impurities, indicative of lignin and hemicellulose coverage. After the isolation process, the corresponding MCC samples (Figures 3b and 3d) exhibit cleaner and smoother surfaces, and a more fibrillated morphology, confirming the removal of non-cellulosic components and exposure of cellulose microfibrils. Pineapple leaf-derived MCC retains a layered fracture pattern, while banana pseudostem-derived MCC shows greater fibril separation, suggesting variations in fiber structure and treatment efficiency.

The SEM image of cassava stem raw material (Figure 3e) reveals a heterogeneous surface morphology, characterized by irregularly arranged small fragments. This structure is indicative of the presence of non-cellulosic components such as hemicellulose, lignin, and pectin, which encapsulate the cellulose fibers. In contrast, the SEM image of MCC derived from cassava stems (Figure 3g) exhibits a well-organized, highly-ordered fibrous structure, characteristic of purified cellulose. This morphological transition provides clear evidence of the high crystallinity achieved in the cassava stem-derived MCC sample.

In the SEM image of the raw spent coffee grounds (Figure 3h), the surface appears rough and heterogeneous, with no visible typical lignocellulosic fiber structures, thus evidencing surface impurities and non-cellulosic residues.

In contrast, the SEM image of the microcrystalline cellulose obtained from spent coffee grounds (Figure 3k)

Figure 2. *MCC extraction steps from various raw materials: from top to bottom - pineapple leaves, banana pseudostems, cassava stems, spent coffee grounds; from left to right - raw material powder, after lignin removal, after bleaching, and final MCC product.*

reveals a much smoother surface morphology with less densely packed microfibrils. These fibrils appear to be well-isolated from each other, indicating the breakdown into discrete cellulose microcrystals after chemical treatment. This morphological change confirms effective removal of hemicellulose, lignin, and surface impurities, while preserving a smooth, ordered cellulose structure.

According to the literature, acid hydrolysis attacks the amorphous regions of cellulose, breaking down the polymer into isolated microcrystals. The penetration of acid ions into fiber interiors promotes depolymerization, particularly in the amorphous regions, while the crystalline domains remain intact.

The average diameter of chemically treated cellulose microcrystals has been reported to be approximately 2 - 3 µm [11]. However, precise length measurements remain challenging due to irregular fragment shapes and overlapping fibrils observed in SEM images.

Notably, the microcrystals extracted from spent coffee grounds are smaller in diameter compared to those reported from other biomass sources. For instance, MCC derived from durian rind shows particle sizes ranging from 6.2 to ~25.4 µm [12], while MCC from date seeds can reach up to 65.3 µm in peak size [13]. The significantly smaller size extracted from spent coffee grounds suggests a more effective hydrolytic breakdown, likely due to a less rigid cell wall structure and efficient chemical processing.

Overall, the morphological changes observed in the SEM images confirm the successful breakdown of the complex lignocellulosic structure and the enrichment of the cellulose phase, which is essential for obtaining MCC suitable for polymer composites or biodegradable plastic applications.

The FTIR spectra of MCC from all four sources (Figure 4) show characteristic cellulose bands, including broad O–H stretching (~3,270 – 3,333 cm^{-1}), C–H stretching (~2,900 cm^{-1}), C–O–C and C–O stretching (1,150 - 1,030 cm^{-1}), and crystalline cellulose peaks at ~1,420 and 895 cm^{-1}. The raw materials display additional signals from non-cellulosic components, such as hemicellulose, lignin, and pectin, which are significantly diminished or absent in the MCC samples, confirming effective purification. Notably, the O–H stretching band in spent coffee ground MCC appears at a lower wavenumber (~3,112 cm^{-1}) compared to ~3,270 – 3,333 cm^{-1} in other MCCs, indicating stronger hydrogen bonding within the cellulose network. This red shift is likely due to the smaller crystallite size and denser packing of cellulose fibrils after treatment, promoting more extensive intermolecular hydrogen bonding.

Figure 5 presents the thermogravimetric (TG) and differential thermal analysis (DTA) curves of MCC derived from pineapple leaves, banana pseudostems, cassava stems, and spent coffee grounds. The thermal degradation profiles of all samples exhibit three distinct mass-loss stages, consistent with previous reports on MCC extracted from lignocellulosic biomass [14, 15].

The first stage, occurring between 30 and 200°C, corresponds to the removal of adsorbed moisture and loosely bound volatiles, with mass losses of 2.37%, 3.88%,

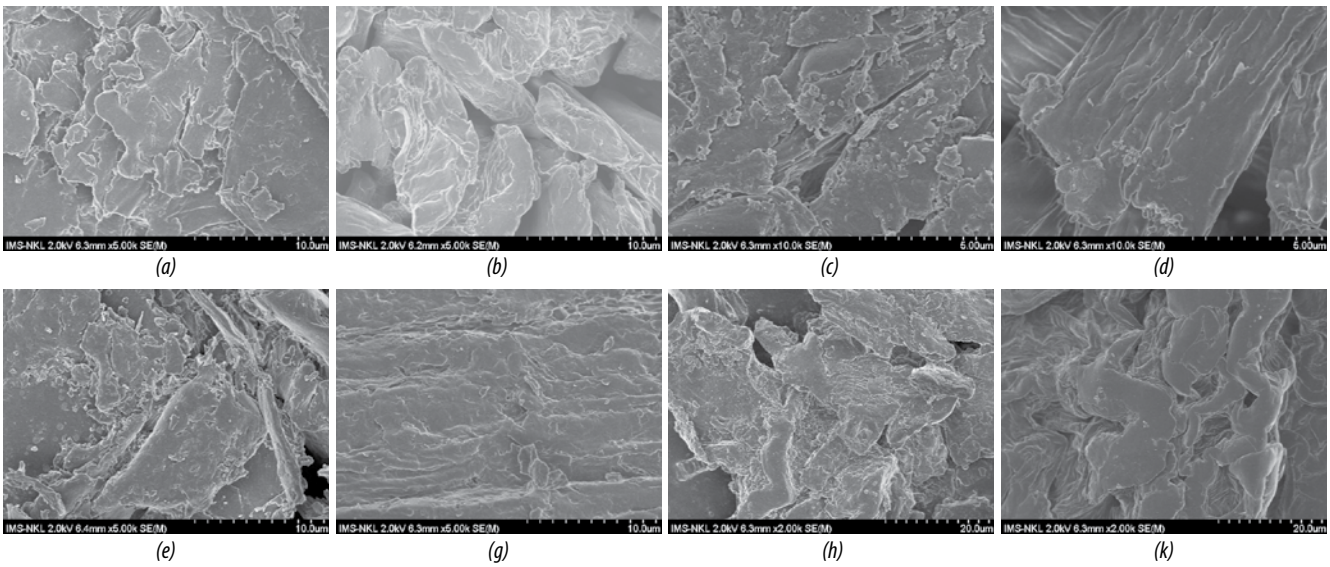

Figure 3. *SEM images of raw materials - pineapple leaves (a), banana pseudostems (c), cassava stems (e), spent coffee grounds (h) - and their corresponding MCC products: pineapple leaves (b), banana pseudostems (d), cassava stems (g), and spent coffee grounds (k).*

4.92%, and 9.77% for MCC from pineapple leaves, banana pseudostemss, cassava stems, and spent coffee grounds, respectively. These variations reflect differences in hydrophilicity and moisture content among the biomass sources.

The second stage, observed between 200 and 400°C, represents the major decomposition region of cellulose, primarily due to the cleavage of β-1,4-glycosidic linkages in the glucose polymer chain. The corresponding mass losses were 76.54%, 72.20%, 64.47%, and 58.04% for MCC from pineapple leaves, banana pseudostems, cassava stems, and spent coffee grounds, respectively. Sharp DTG peaks appeared at 332.39°C, 336.04°C, 330.65°C, and 316.68°C for these samples, indicating the main pyrolysis temperatures of cellulose. The absence of peaks in the regions of 200 - 280°C (typical of hemicellulose) and 380 - 450°C (typical of lignin) confirms that most hemicellulose and lignin impurities were effectively removed.

The third stage, occurring between 400 and 600°C, involves the secondary decomposition of residual carbonaceous matter and thermally stable lignin fractions, reflecting the remaining non-cellulosic content. The residual mass beyond 600°C was very low (only a few percent), indicating a low ash and inorganic content.

The TGA/DTG profiles indicate that the main decomposition temperatures of MCC isolated from the four biomass sources ranged from 316 to 336°C, with very low residual ash contents. These values are comparable to those reported for MCC derived from other lignocellulosic materials in the literature [16, 17].

Collectively, the TG-DTA results confirm that the applied preparation processes effectively removed non-cellulosic organic matter and inorganic components, producing MCC with high thermal stability and purity across all four biomass sources.

The XRD patterns of the raw materials and the MCC

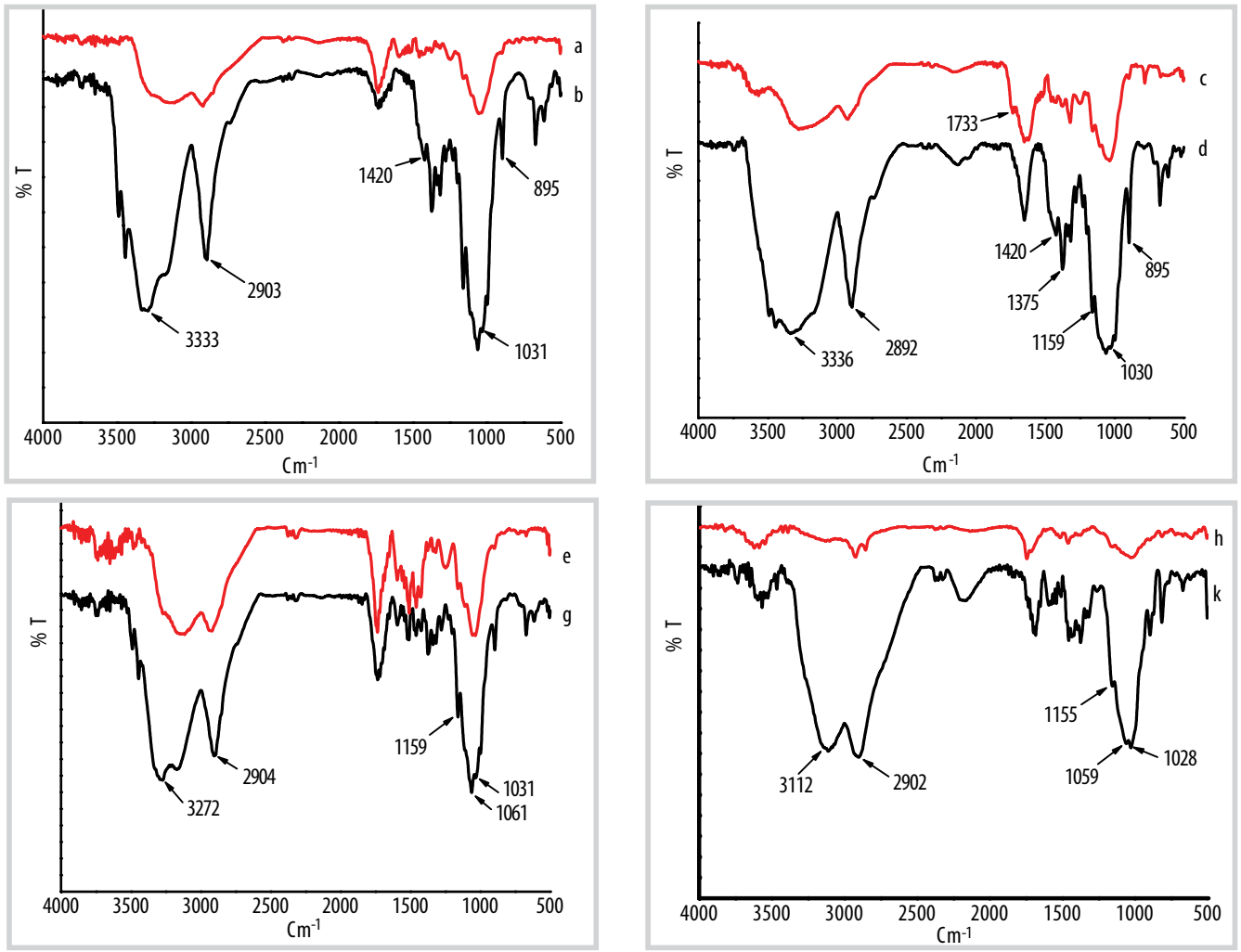

Figure 4. *FTIR spectra of raw materials - pineapple leaves (a), banana pseudostems (c), cassava stem (e), and spent coffee grounds (h) - and their corresponding MCC samples.*

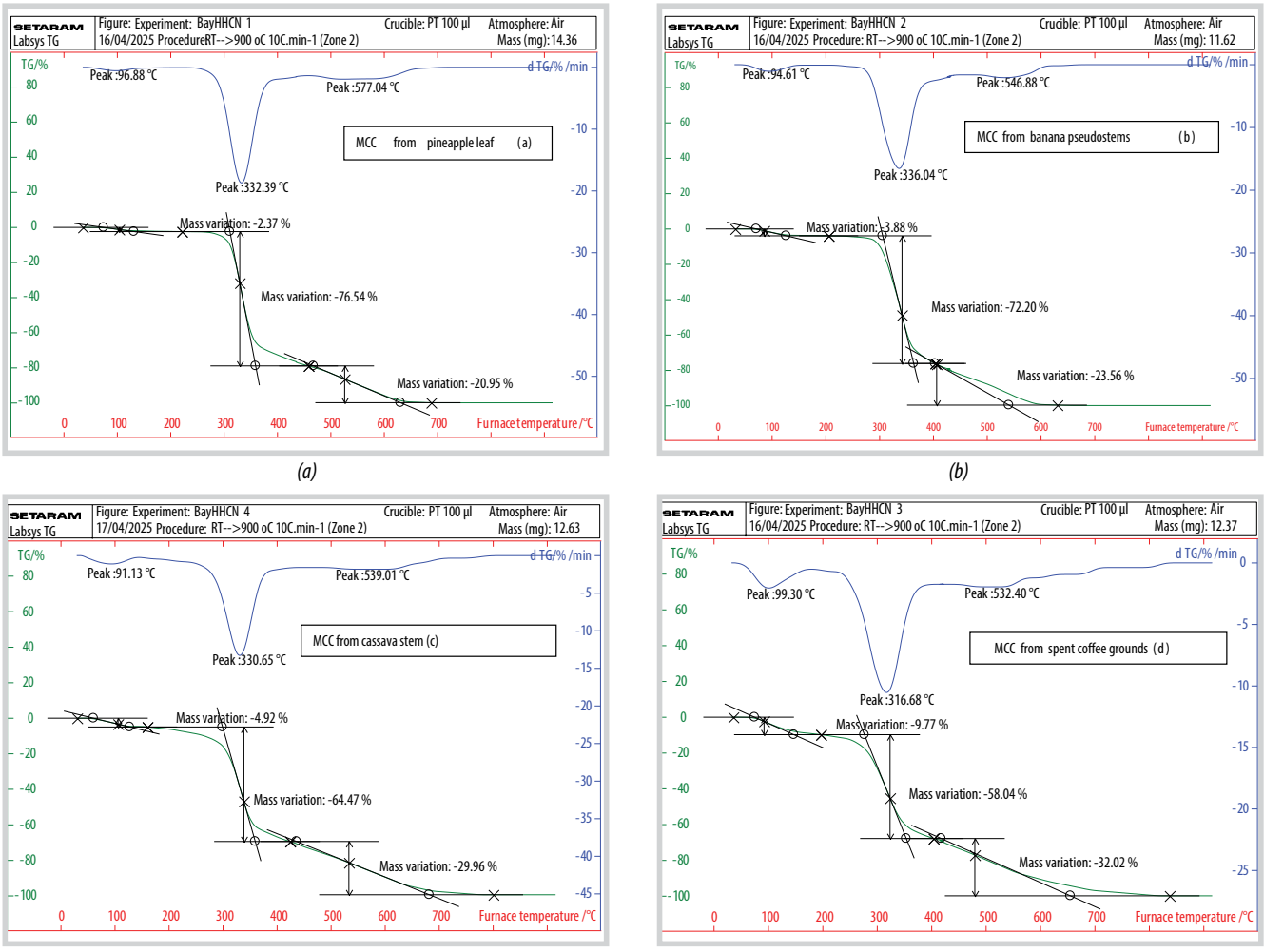

Figure 5. *Thermogravimetric (TG) and differential thermal analysis (DTA) curves of MCCs derived from four biomass sources: (a) pineapple leaves, (b) banana pseudostems, (c) cassava stem, and (d) spent coffee grounds.*

Table 3. *Crystallinity index (CrI) and crystal size of raw biomass samples and corresponding MCC*

No.	Sample name	Crystalline index (CrI, %)	Crystal size (nm)
1	Raw pineapple leaves	37.5	2.19
	MCC from pineapple leaves	73.1	4.58
2	Raw banana pseudostems	48.1	2.09
	MCC from banana pseudostems	63.4	4.61
3	Raw cassava stems	56.7	2.31
	MCC from cassava stems	74.8	4.18
4	Raw spent coffee grounds	29.4	2.82
	MCC from spent coffee grounds	69.2	4.34

obtained from four biomass sources - (a) pineapple leaves, (b) banana pseudostems, (c) cassava stems, and (d) spent coffee grounds - are shown in Figure 6. The corresponding crystallinity index (CrI) and crystal size values of the samples are summarized in Table 3.

The amorphous (I_{am}) and crystalline (I_{002}) diffraction peaks were observed in the 2θ ranges of 16.01° - 16.8° and 22.1° - 22.8°, respectively (Figure 6). As shown in the results table, all samples exhibited increased crystallinity index and crystal size after the preparation process. The variations in peak height and width among the samples reflected differences in crystallinity degree and crystal size [18]. The higher CrI value of the MCC samples compared to their corresponding raw materials can be attributed to

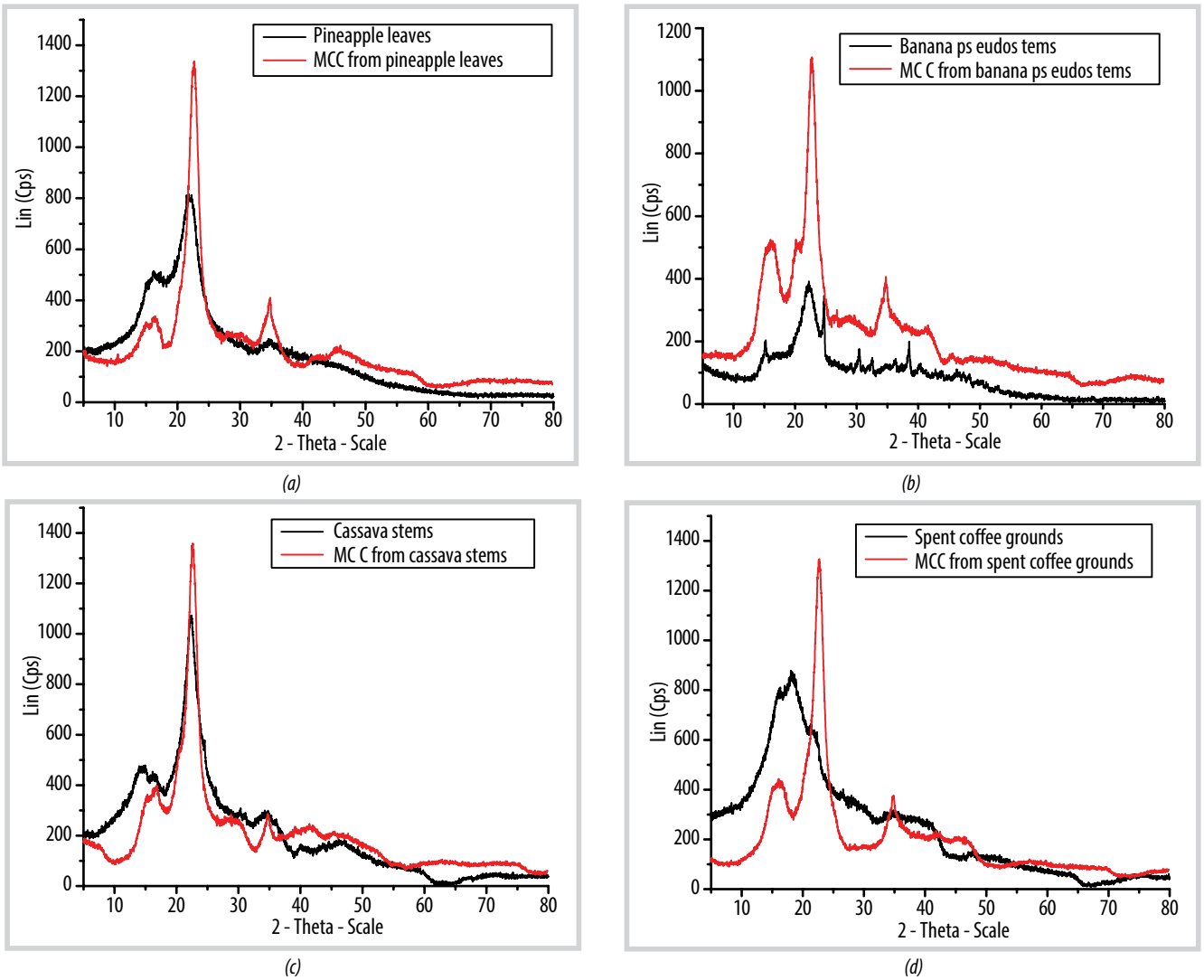

Figure 6. *XRD patterns of raw materials and the corresponding MCC obtained from four biomass sources: pineapple leaves (a), banana pseudostems (b), cassava stems (c), and spent coffee grounds (d).*

the removal of amorphous cellulose regions during acid hydrolysis, which cleaves the 1,4-glycosidic bonds.

Overall, the MCC extracted from cassava stems, banana pseudostems, pineapple leaves, and spent coffee grounds demonstrated distinct differences in yield, particle morphology, crystallinity, and thermal stability. Among these, cassava stems possessed a relatively high cellulose content and MCC recovery efficiency, second only to pineapple leaves. Moreover, cassava stems are widely available across Vietnam - from North to South - particularly in provinces such as Tay Ninh province, Gia Lai province, Dak Lak province, Quang Ngai province, Dong Nai province, Nghe An province, Phu Tho province, and Son La province. Therefore, MCC derived from cassava stems offers the most favorable combination of recovery yield, particle uniformity, crystallinity index, and thermal stability. Given both its material performance and the abundance of feedstock, cassava stem-derived MCC is the most practical and sustainable source for large-scale production. Consequently, it was selected for subsequent composite fabrication with TPS and PLA to ensure optimal reinforcement efficiency and processing stability.

3.2. Structural, thermal, and morphological analysis of MCC-reinforced TPS/PLA composites

3.2.1. X-ray diffraction

The XRD pattern of the PLA sample (Figure 7a) exhibited characteristic diffraction peaks at 2θ ≈ 16.8°, 19.1°, 22.6°, and 28.9°. The most intense diffraction peak at 2θ = 16.8° corresponds to the (200)/(110) lattice planes, confirming the predominance of the α-form crystalline phase of PLA, which is known to be the thermodynamically most stable crystalline modification of polylactic acid.

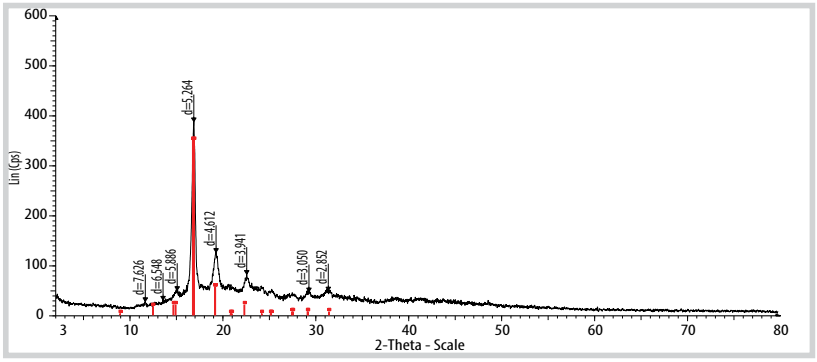

(a)

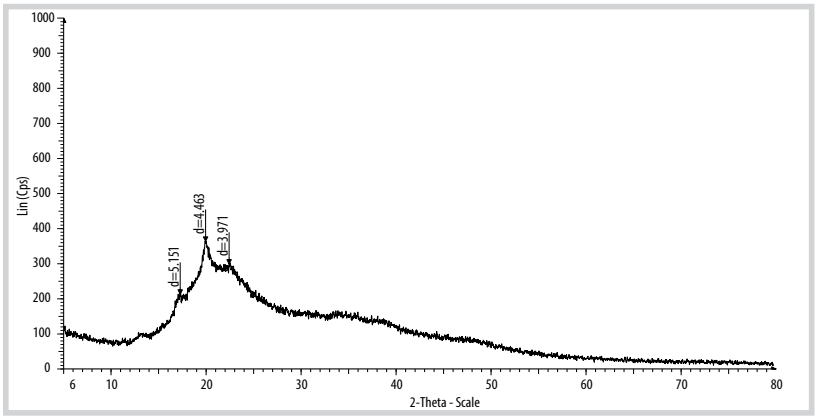

(b)

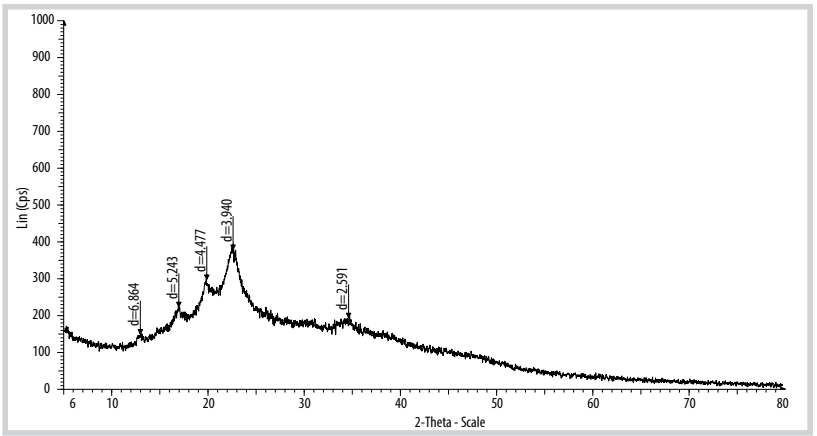

(c)

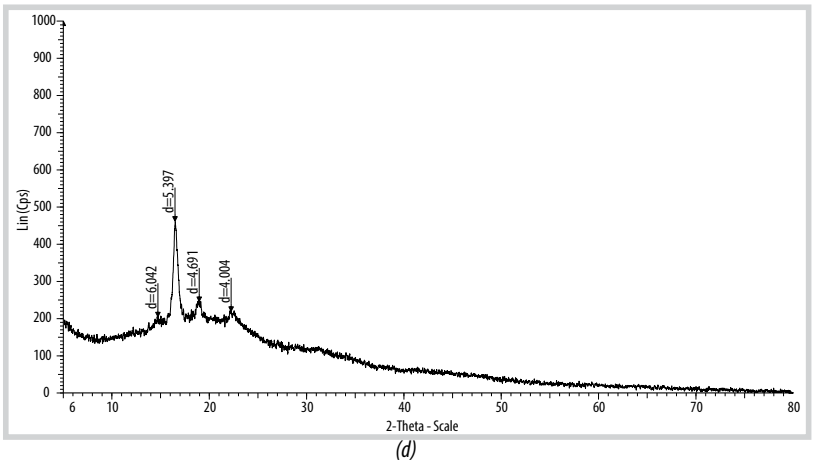

(d)

Figure 7. *X-ray diffraction patterns of (a) PLA, (b) thermoplastic starch (TPS), (c) MCC/TPS, and (d) PLA/(MCC/TPS) composites.*

Upon thermoplasticization with glycerol and water, the TPS (Figure 7b) sample showed a substantial reduction or complete disappearance of these crystalline peaks, replaced by a broad amorphous halo at 2θ ≈ 17° - 22.5°, confirming the disruption of the semi-crystalline starch structure during gelatinization and melt processing.

In the MCC/TPS composite (Figure 7c), the amorphous halo of TPS remained, while characteristic cellulose I peaks of MCC at 2θ ≈ 16.0°, 22.5°, and 34.5° appeared with increased intensity, resulting in a higher overall crystallinity. This confirms MCC's role as a crystalline reinforcing phase dispersed within the amorphous TPS matrix.

For PLA/(MCC/TPS) composites (Figure 7d), diffraction peaks at 2θ ≈ 15°, 16.5°, 19°, and 22.5° were observed, corresponding to PLA's crystalline structure alongside the amorphous halo of TPS and MCC peaks. The coexistence of these crystalline and amorphous domains suggests a multiphase morphology without complete miscibility among the components.

3.2.2. Thermal analysis

The TGA/DTG results revealed that the TPS, MCC/TPS, and PLA/(MCC/TPS) samples exhibited two main stages of mass losss with increasing temperature. The first stage (below 200°C) corresponds to the evaporation of moisture and partial volatilization of glycerol-rich phases, with weight losses of 11.39%, 10.55%, and 15.16% for TPS, MCC/TPS, and PLA/(MCC/TPS), respectively. In contrast, the mass of the PLA sample remained nearly constant in this region, confirming its high thermal stability and the absence of chemical degradation.

The second stage (200 - 600°C) is associated with the thermal degradation of starch-rich phases, overlapping with the decomposition of MCC. The major

weight losses were 88.56% for TPS, 89.03% for MCC/TPS, and 84.78% for PLA/(MCC/TPS), with corresponding DTA peaks at 315.02°C, 326.84°C, and 348.55°C. This stage highlights the difference in degradation mechanisms between PLA and starch/cellulose-based systems. Pure PLA underwent a single major decomposition step at 355.69°C, resulting in a mass loss of approximately 87.99%. The lower degradation temperatures observed for TPS, MCC/TPS, and PLA/(MCC/TPS) compared to pure PLA indicate that incorporating MCC/TPS into the PLA matrix increased the residual char yield and slightly reduced the decomposition temperature. These effects reflect the influence of interfacial interactions and the degree of MCC dispersion within the PLA matrix on the overall thermal stability of the composites.

3.2.3 Morphological analysis (SEM)

The SEM image of neat PLA (Figure 9a) shows a relatively smooth and dense surface with slight roughness, indicating the coexistence of amorphous and crystalline regions. No visible cracks or phase separation are observed, confirming the good morphological stability of pure PLA.

In contrast, the TPS sample (Figure 9b) displays a rough and irregular surface with micro-voids and discontinuities, suggesting incomplete gelatinization and partial incompatibility between starch and the plasticizer. For the MCC/TPS composite (Figure 9c), bright particles corresponding to MCC are observed partially embedded in the starch matrix, indicating non-uniform dispersion and partial aggregation of MCC.

The PLA/(MCC/TPS) composites (Figure 9d) exhibit smoother and more compact fracture surfaces, implying finer dispersion and improved compatibility between PLA and TPS. This enhancement is likely due to branching and crosslinking reactions between maleic anhydride–modified PLA (PLA-MA) and hydroxyl groups of starch, which reduce interfacial tension and improve miscibility at the polymer–filler interface.

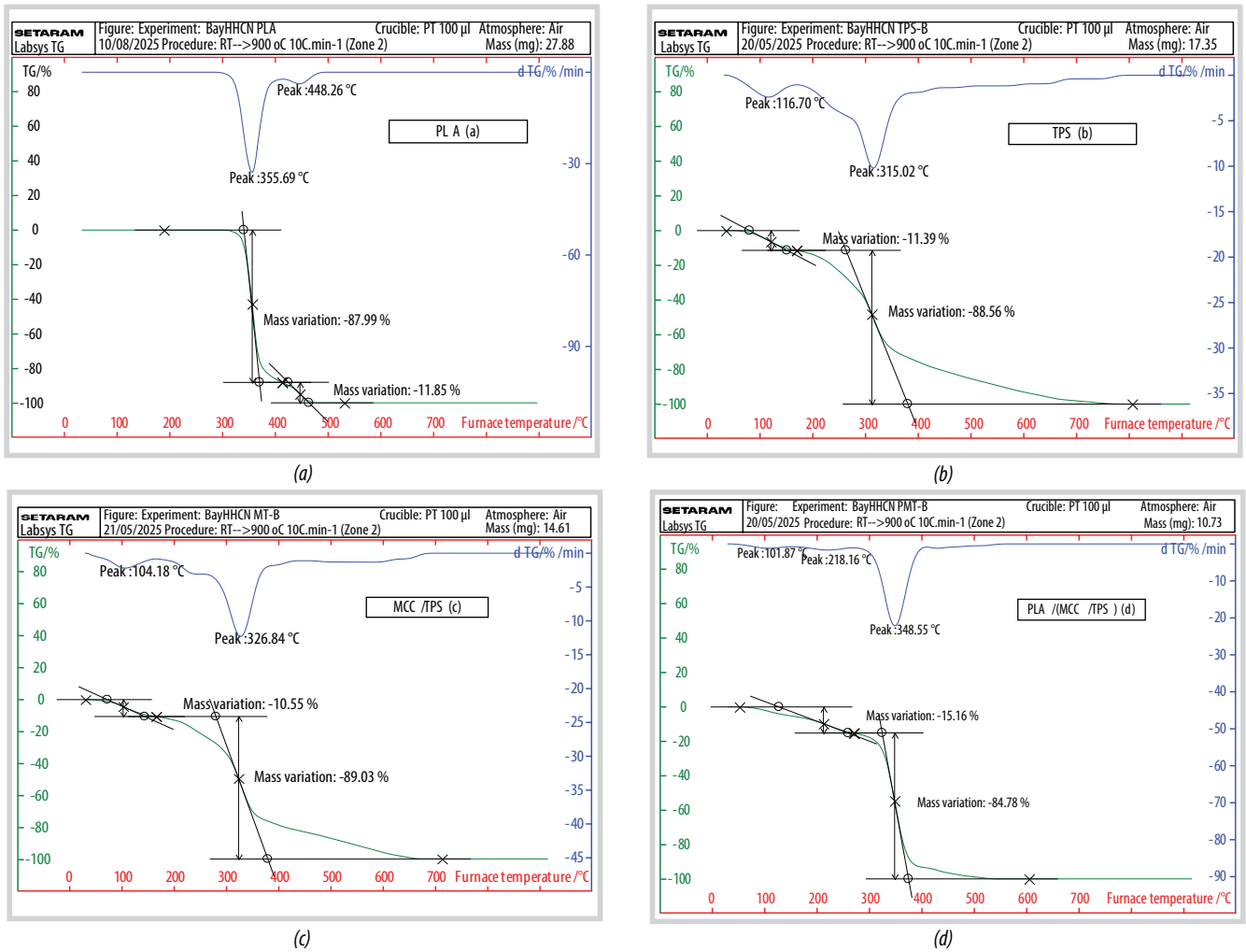

Figure 8. *TG-DTA thermal analysis curves of (a) PLA, (b) TPS, (c) MCC/TPS, and (d) PLA/(MCC/TPS) composites.*

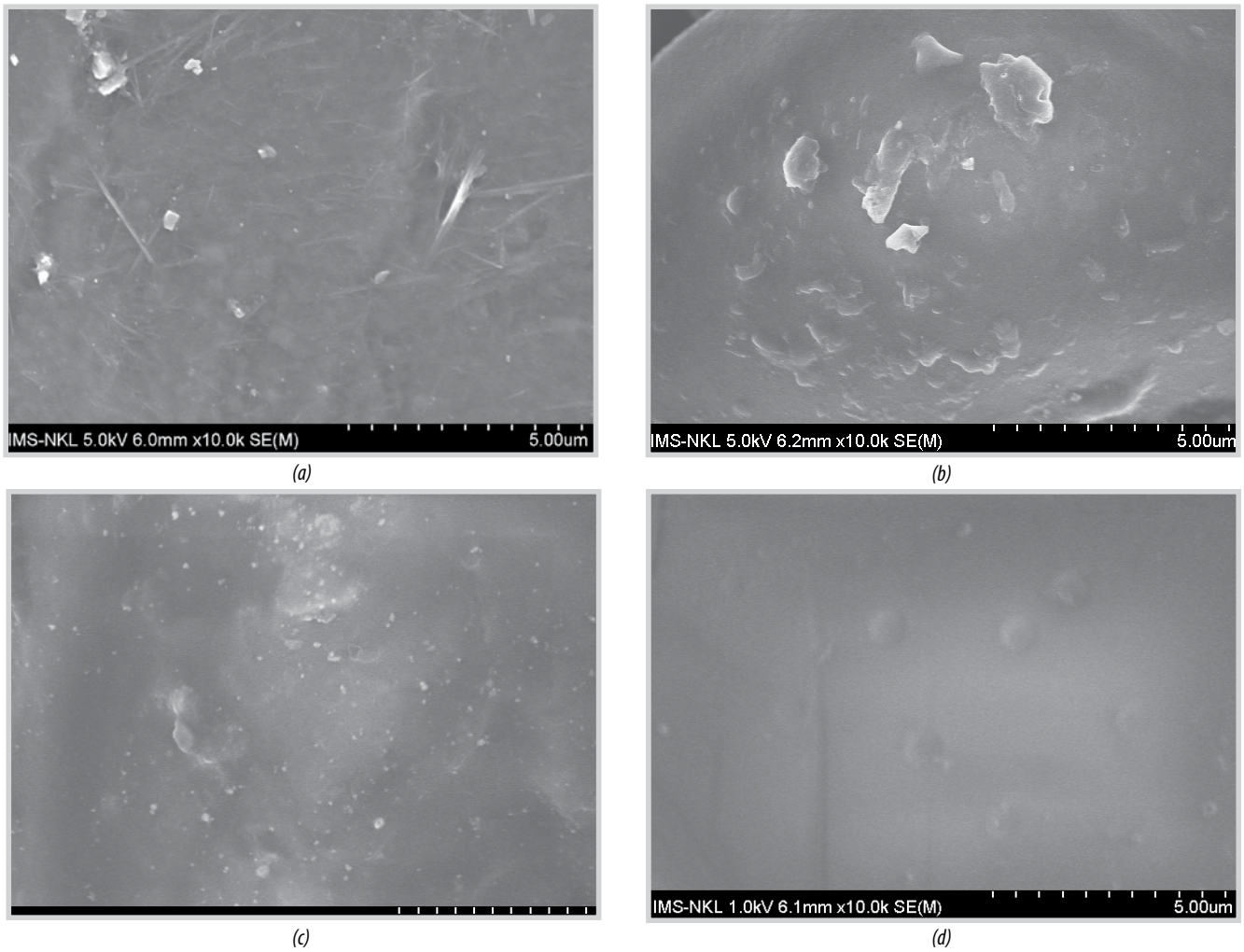

Figure 9. *Scanning electron microscopy (SEM) images of (a) PLA, (b) TPS, (c) MCC/TPS, and (d) PLA/(MCC/TPS) composites.*

These morphological findings support the hypothesis that well-dispersed MCC (≤15 wt%) enhances interfacial bonding and mechanical reinforcement, whereas excessive MCC loading (≈20 wt%) tends to induce particle agglomeration, decreasing composite uniformity and ductility.

3.3. Mechanical properties of PLA/(MCC/TPS) composites

Table 4 summarizes the tensile strength, elongation at break, and elastic modulus of the composites. Increasing TPS and MCC content led to a progressive decrease in tensile strength and elongation, consistent with the reduction of PLA's reinforcing fraction.

The B70:4.5:25.5 formulation (PLA:MCC:TPS = 70:4.5:25.5), corresponding to 15 wt% MCC in the MCC/TPS blend, exhibited the best balance of mechanical performance and biodegradability, making it suitable for packaging or food tray applications. The observed mechanical trends were consistent with the structural and morphological analyses, where SEM images revealed that improved MCC dispersion enhanced the tensile strength relative to pure PLA. TGA/DTA results indicated greater thermal stability, contributing to improved durability during melt processing. XRD analysis confirmed the presence of crystalline MCC, which increased the stiffness of the composites. However, excessive MCC loading led to embrittlement, emphasizing the need for optimized filler content.

4. Conclusions

Microcrystalline cellulose was extracted from cassava stems, banana pseudostems, pineapple leaves, and spent coffee grounds. Among these sources, cassava stem MCC was identified as the most feasible and sustainable source due to its high crystallinity, uniform particle dimensions, processing stability, ready availability, and large-scale supply potential. This MCC was subsequently incorporated into thermoplastic starch and polylactic acid matrices

Table 4. *Mechanical properties of the composite materials.*

Sample	Tensile strength (MPa)	Elongation at break (%)	Elastic modulus (MPa)
A80:2:18	41.2	7.1	1980
A70:3:27	35.0	6.3	1725
B70:4.5:25.5	32.5	5.5	1850
B60:6:34	29.2	4.1	1900
C60:8:32	25.5	3.2	2000
PLA	45	3.5	2500

to produce fully biodegradable composites. Structural, morphological, and thermal analyses confirmed that well-dispersed MCC acts as an effective reinforcing phase, enhancing tensile strength, elastic modulus, and thermal stability. The optimized PLA:MCC:TPS ratio of 70:4.5:25.5 (corresponding to 15 wt% MCC in the MCC/TPS blend) achieved the best balance between mechanical performance and biodegradability, making the resulting composites suitable for sustainable packaging and food service applications. These findings align with global energy transition strategies and CO_2 mitigation objectives, offering a viable pathway to replace petrochemical-based plastics in targeted sectors.

References

[1] K.O. Reddy, C. Uma Maheswari, E. Muzenda, M. Shukla, and A.V. Rajulu, "Extraction and characterization of cellulose from pretreated ficus (peepal tree) leaf fibers", *Journal of Natural Fibers*, Volume 13, Issue 1, pp. 54 - 64, 2016.

[2] Naved Azum, Mohammad Jawaid, Lau, Kia Kian, Anish Khan, and Maha Moteb Alotaibi, "Extraction of microcrystalline cellulose from Washingtonia fibre and its characterization", *Polymers*, Volume 13, Issue 18, 2021. DOI: 10.3390/polym13183030.

[3] C. Uma Maheswari, K. Obi Reddy, E. Muzenda, B. Guduri, and A. Varada Rajulu, "Extraction and characterization of cellulose microfibrils from agricultural residue - Cocos nucifera L", *Biomass and Bioenergy*, Volume 46, pp. 555 - 563, 2012. DOI: 10.1016/j.biombioe.2012.06.039.

[4] P. Nehra and R.P. Chauhan, "Facile synthesis of nanocellulose from wheat straw as an agricultural waste", *Iranian Polymer Journal*, Volume 31, Issue 6, pp. 771 - 778, 2022. DOI:10.1007/s13726-022-01040-0.

[5] Mohd Yussni Hashim, Azriszul Mohd Amin, Omar Mohd Faizan Marwah, Mohd Hilmi Othman, Mohd Radzi Mohamed Yunus, and Ng Chuan Huat, "The effect of alkali treatment under various conditions on physical properties of kenaf fiber", *Journal of Physics: Conference Series*, Volume 914, 2017. DOI: 10.1088/1742-6596/914/1/012030.

[6] Selwin Maria Sekar, Rajini Nagarajan, Ponsuriyaprakash Selvakumar, Nadir Ayrilmis, Kumar Krishnan, Faruq Mohammad, Hamad A. Al-Lohedan, and Sikiru O. Ismail, "3D-printed green biocomposites from poly(lactic acid) and pine wood-derived microcrystalline cellulose: Characterization and properties", *BioResources*, Volume 20, Issue 4, pp. 8473 - 8492, 2025. DOI: 10.15376/biores.20.4.8473-8492.

[7] M.K. Mohamad Haafiz, Azman Hassan, Zainoha Zakaria, I.M. Inuwa, M.S. Islam, M. Jawaid, "Properties of polylactic acid composites reinforced with oil palm biomass microcrystalline cellulose", *Carbohydrate Polymers*, Volume 98, Issue 1, 15, pp. 139 - 145, 2013.

[8] Nanang Triyono, Fatma Sari, Ika Kurniaty, Ratri Ariatmi Nugrahani, Tri Yuni Hendrawati, and Susanty, "Characterization of microcrystalline cellulose from cassava stems through acid hydrolysis process using H_2SO_4 with variation concentration", *International Conference on Engineering, Construction, Renewable Energy, and Advanced Materials, Fakultas Teknik Universitas Muhammadiyah Jakarta, 30 April 2024*.

[9] Jie Chen, Xia Wang, Zhu Long, Shuangfei Wang, Jingxian Zhang, and Lei Wang, "Preparation and performance of thermoplastic starch and microcrystalline cellulose for packaging composites: Extrusion and hot pressing", *International Journal of Biological Macromolecules*, Volume 165, pp. 2295 - 2302, 2020. DOI: 10.1016/j.ijbiomac.2020.10.117.

[10] Daniele Rigotti, Luca Fambri, Alessandro Pegoretti, "Bio composites for fused filament fabrication: effects of maleic anhydride grafting on poly(lactic acid) and microcellulose", *Progress in Additive Manufacturing*, Volume 7, pp. 765 - 783, 2022. DOI: 10.1007/s40964-022-00264-z.

[11] Nehemiah Mengistu Zeleke, Devendra Kumar Sinha, and Getinet Asrat Mengesha, "Chemical composition and extraction of micro crystalline cellulose from outer skin isolated coffee husk", *Advances in Materials Science and Engineering*, 2022. DOI: 10.1155/2022/7163359.

[12] Wei Sing Yong, Yee Lee Yeu, Ping Ping Chung, and Kok Heng Soon, "Extraction and characterization of microcrystalline cellulose (MCC) from durian rind for biocomposite application", *Journal of Polymers and the Environment*, Volume 32, pp. 6544 - 6575, 2024. DOI: 10.1007/s10924-024-03401-7.

[13] Yanlan Liu, Jingfeng Ran, Ziyang Xu, Hao Cheng, Benping Lin, Tianran Deng, and Cuiping Yi, "Preparation and characterization of microcrystalline cellulose from rice bran", *Journal of the Science of Food and Agriculture*, Volume 105, Issue1, pp. 218 - 226, 2025. DOI: 10.1002/jsfa.13820.

[14] Xutong Wang, Xiaoqiang Cui, Yuechi Che, Shengquan Zhou, Zeng Dan, Beibei Yan, Guanyi Chen, and Ting Wang, "Gasification of Tibetan herb residue: Thermogravimetric analysis and experimental study", *Biomass and Bioenergy*, Volume 146, 2021. DOI: 10.1016/j.biombioe.2020.105952.

[15] Raquel S. Reis, Lucas G.P. Tienne, Diego de H.S. Souza, Maria de Fátima V. Marques, and Sergio N. Monteiro, "Characterization of coffee parchment and innovative steam explosion treatment to obtain micro - brillated cellulose as potential composite reinforcement", *Journal of Materials Research and Technology*, Volume 9, Issue 4, pp. 9412 - 9421, 2020. DOI: 10.1016/j.jmrt.2020.05.099.

[16] Putri Nawangsari, Warman Fatra, Aryandi Kusuma, Muftil Badri, Dedi Rosa P.C, and Dedy Masnur, "Microcellulose from pineapple leaf Fiber as a potential sustainable material: Extraction and characterization", *Journal Polimesin*, Volume 22, Issue 1, 2024.

[17] Sataporn Malarat, Dilawin Khongpun, Kanokkorn Limtong, Napasin Sinthuwong, Pornpinun Soontornapaluk, Chularat Sakdaronnarong, and Pattaraporn Posoknistakul, "Preparation of nanocellulose from coffee pulp and its potential as a polymer reinforcement", *ACS Omega*, Volume 8, Issue 28, pp. 25122 - 25133, 2023. DOI: 10.1021/acsomega.3c02016.

[18] Djalal Trache, André Donnot, Kamel Khimeche, Riad Benelmir, and Nicolas Brosse, "Physico-chemical properties and thermal stability of microcrystalline cellulose isolated from alfa fibres", *Carbohydrate Polymers*, Volume 104, pp. 223 - 230. 2014. DOI: 10.1016/j.carbpol.2014.01.058.